Cell Reports, Volume *33*

Supplemental Information

Enhancer Reprogramming Confers Dependence on Glycolysis and IGF Signaling in KMT2D Mutant Melanoma

Mayinuer Maitituoheti, Emily Z. Keung, Ming Tang, Liang Yan, Hunain Alam, Guangchun Han, Anand K. Singh, Ayush T. Raman, Christopher Terranova, Sharmistha Sarkar, Elias Orouji, Samir B. Amin, Sneha Sharma, Maura Williams, Neha S. Samant, Mayura Dhamdhere, Norman Zheng, Tara Shah, Amiksha Shah, Jacob B. Axelrad, Nazanin E. Anvar, Yu-Hsi Lin, Shan Jiang, Edward Q. Chang, Davis R. Ingram, Wei-Lien Wang, Alexander Lazar, Min Gyu Lee, Florian Muller, Linghua Wang, Haoqiang Ying, and Kunal Rai

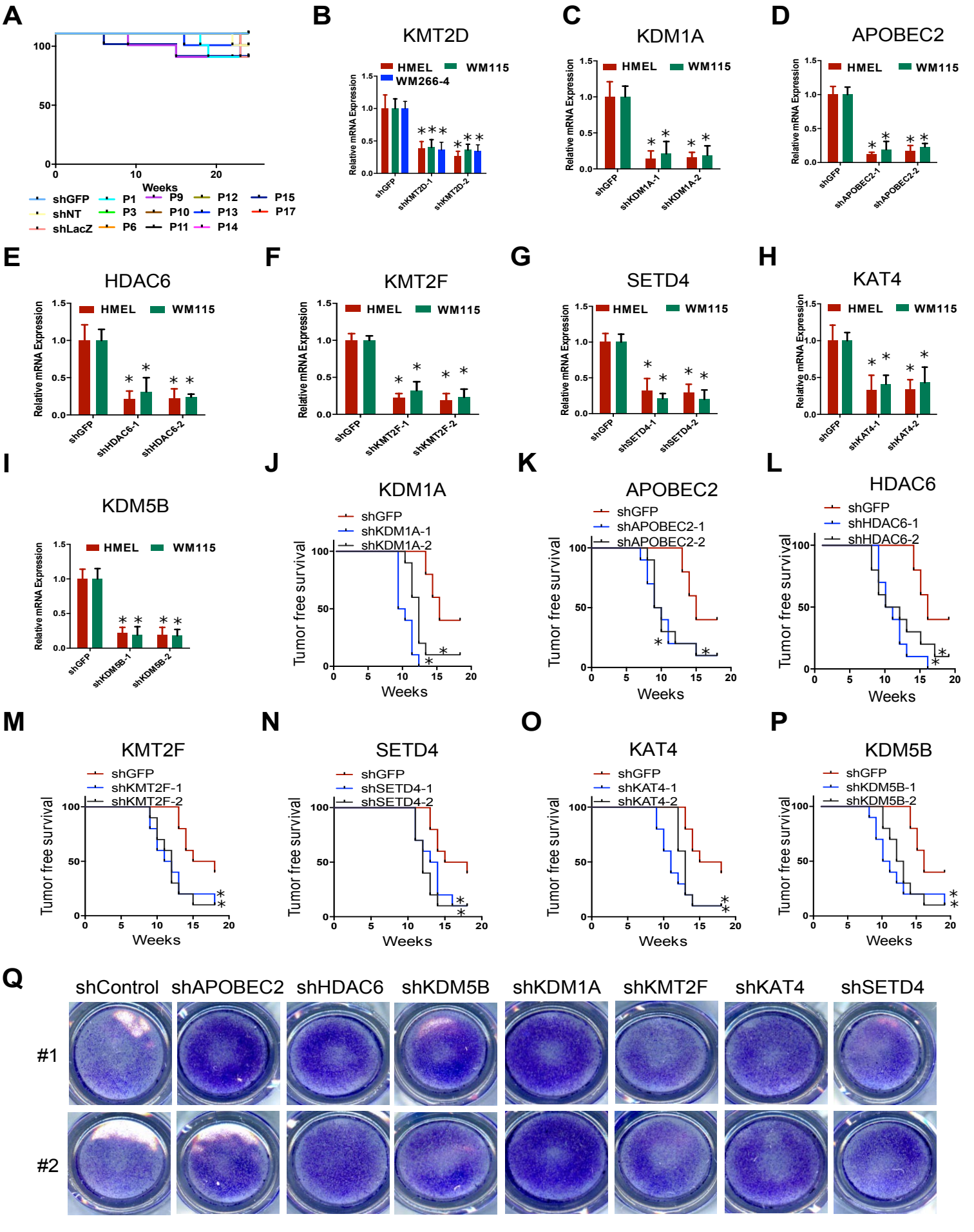
A
Weeks
shGFP
shNT
shLacZ
P1
P3
P6
P9
P10
P11
P12
P13
P14
P15
P17
B
KMT2D
HMEL
WM115
WM266-4
Relative mRNA Expression
shGFP
shKMT2D-1
shKMT2D-2
C
KDM1A
shKDM1A-1
shKDM1A-2
D
APOBEC2
shAPOBEC2-1
shAPOBEC2-2
E
HDAC6
shHDAC6-1
shHDAC6-2
F
KMT2F
shKMT2F-1
shKMT2F-2
G
SETD4
shSETD4-1
shSETD4-2
H
KAT4
shKAT4-1
shKAT4-2
I
KDM5B
shKDM5B-1
shKDM5B-2
J
KDM1A
Tumor free survival
Weeks
shGFP
shKDM1A-1
shKDM1A-2
K
APOBEC2
shAPOBEC2-1
shAPOBEC2-2
L
HDAC6
shHDAC6-1
shHDAC6-2
M
KMT2F
shKMT2F-1
shKMT2F-2
N
SETD4
shSETD4-1
shSETD4-2
O
KAT4
shKAT4-1
shKAT4-2
P
KDM5B
shKDM5B-1
shKDM5B-2
Q
shControl
shAPOBEC2
shHDAC6
shKDM5B
shKDM1A
shKMT2F
shKAT4
shSETD4
#1
#2

Figure S1, related to **Figure1: Validation of epigenetic regulators identified through RNAi screen identified 8 epigenetic regulators as potential tumor suppressors in melanoma.** (**A)** Kaplan-Meier curve showing tumor-free survival of mouse cohorts orthotopically injected with 1 million HMEL-BRAF^{v600E} cells (per flank) that are transfected with pooled shRNAs from primary screen. This figure shows data from pools that did not significantly accelerate tumorigenesis. Three negative control pools (shLuc, shGFP and shNT) are shown. Cells from each pool were injected in 10 mice each and tumor formation was monitored over 25 weeks. (**B-I)** Bar graph showing relative levels (n=3) of indicated genes in the HMEL-BRAF^{V600E} and WM115 cells harboring lentivirally integrated shRNAs for that gene or GFP. Y-axis represents fold change of the gene expression compared to 28s and normalized to control shRNA samples. Data are presented as the mean ± SEM (error bars) of at least three independent experiments or biological replicates. Standard t-test *p < 0.05, **p < 0.01, ***p < 0.001. (**J-P)** Kaplan-Meier curve showing tumor-free survival of mouse cohorts orthotopically injected with WM115 cells stably expressing shRNAs against KDM1A (**J**), APOBEC2 (**K**), HDAC6 (**L**), KMT2F (**M**), SETD4 (**N**), KAT4 (**O**) and KDM5B (**P**). Mantel-cox test *p < 0.05, **p < 0.01, and ***p<0.001 ; n = 10 per arm. **(Q)** Representative images for invaded cells from Boyden chamber assay of HMEL-BRAF^{V600E} cells harboring lentivirally integrated shRNAs for GFP (control) or APOBEC2, HDAC6, KDM5B, KDM1A, SETD4, KMT2F or KAT4. #1 and #2 represent the duplicates for the experiment.

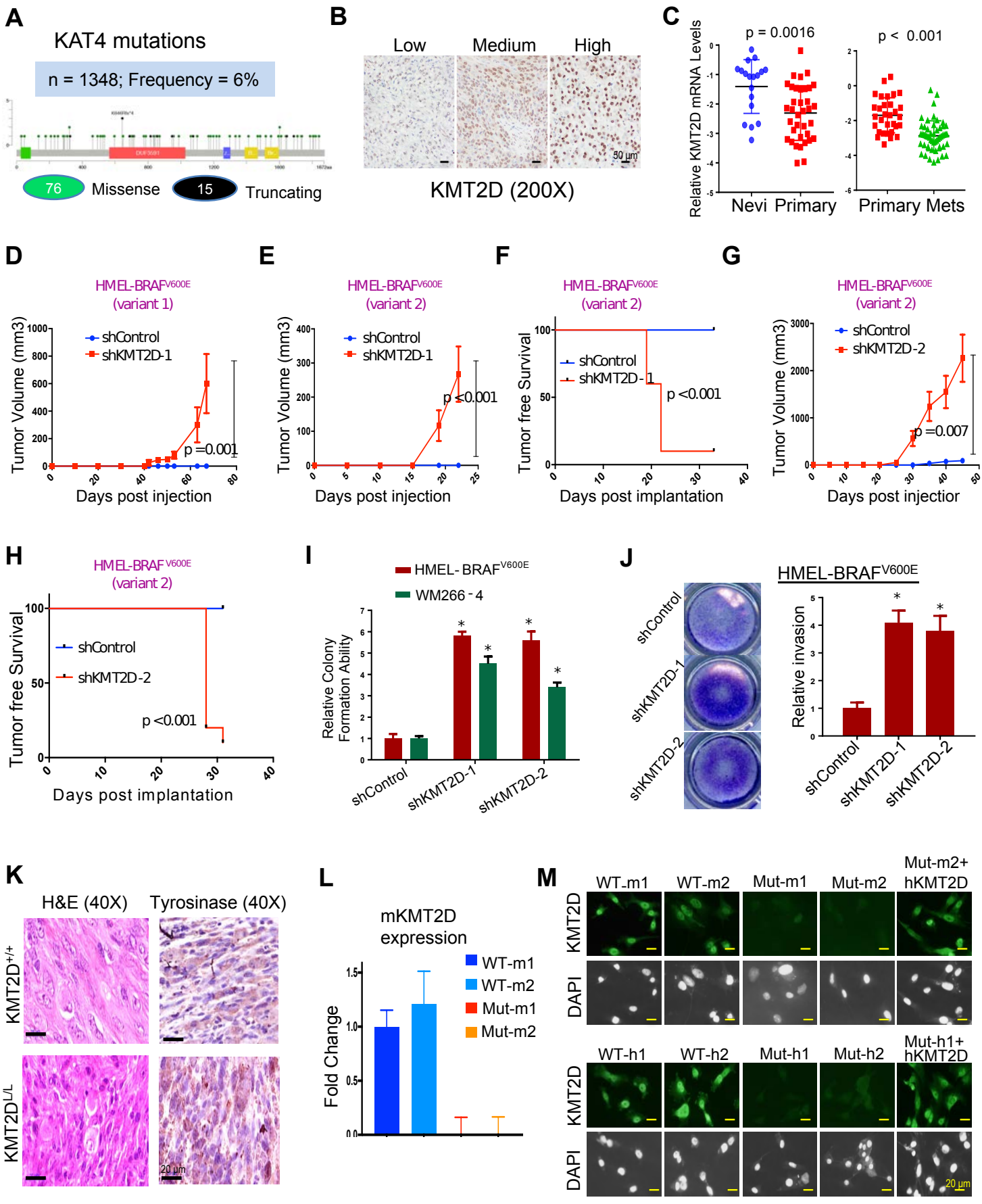
A
KAT4 mutations
n = 1348; Frequency = 6%
76
Missense
15
Truncating
B
Low
Medium
High
50 µm
KMT2D (200X)
C
p = 0.0016
p < 0.001
Relative KMT2D mRNA Levels
Nevi
Primary
Primary Mets
D
HMEL-BRAFV600E
(variant 1)
shControl
shKMT2D-1
Tumor Volume (mm3)
p =0.001
Days post injection
E
HMEL-BRAFV600E
(variant 2)
shControl
shKMT2D-1
Tumor Volume (mm3)
p <0.001
Days post injection
F
HMEL-BRAFV600E
(variant 2)
Tumor free Survival
shControl
shKMT2D-1
p <0.001
Days post implantation
G
HMEL-BRAFV600E
(variant 2)
shControl
shKMT2D-2
Tumor Volume (mm3)
p =0.007
Days post injection
H
HMEL-BRAFV600E
(variant 2)
Tumor free Survival
shControl
shKMT2D-2
p <0.001
Days post implantation
I
HMEL- BRAFV600E
WM266 - 4
Relative Colony Formation Ability
shControl
shKMT2D-1
shKMT2D-2
J
shControl
shKMT2D-1
shKMT2D-2
HMEL-BRAFV600E
Relative invasion
shControl
shKMT2D-1
shKMT2D-2
K
H&E (40X)
Tyrosinase (40X)
KMT2D+/+
KMT2DL/L
20 µm
L
mKMT2D
expression
WT-m1
WT-m2
Mut-m1
Mut-m2
Fold Change
M
WT-m1
WT-m2
Mut-m1
Mut-m2
Mut-m2+
hKMT2D
KMT2D
DAPI
WT-h1
WT-h2
Mut-h1
Mut-h2
Mut-h1+
hKMT2D
KMT2D
DAPI
20 µm

Figure S2, related to **Figure 2: Validation of KMT2D as a tumor-suppressor in melanoma.** (**A**) Schematic of KAT4 protein showing missense mutations seen across all melanoma studies deposited in cBio portal. Green filled circles denote missense mutations whereas black filled circles represent truncating mutations. Colored boxes within KAT4 schematic show different protein domains. (**B**) Representative images for KMT2D staining in the human melanoma TMA for which data is shown in Figure 2C. Low, medium and high nuclear intensities of KMT2D are shown. Scale bars represent 50 μm. (**C**) Dot plot showing relative KMT2D mRNA levels between nevi (n=18) and primary melanomas (n=45) (from Talantov et al., 2005) (left panel) and between primary (n=30) and metastatic (n=52) melanomas (from Xu et al., 2008) (right panel). (**D**, **E** and **G**) Graph showing tumor volume (n=5) of HMEL-BRAF^{V600E} cells (clonal variant 1 in panel **D** and clonal variant 2 in panels **E** and **G**) harboring either control (shNT) or KMT2D shRNAs (shKMT2D-1 in panel **E** and KMT2D-2 in panel **G**). (**F** and **H**) Kaplan-Meier curve showing tumor-free survival of mouse cohorts orthotopically injected with HMEL-BRAF^{V600E} cells (clonal variant 2) harboring either control (shNT) or KMT2D shRNAs (shKMT2D-1 in panel **F** and KMT2D-2 in panel **H**), n = 10 per arm. (**I**) Relative soft agar colony formation ability of HMEL-BRAF^{V600E} or WM266-4 cells (n=3) harboring control or 2 different KMT2D shRNAs (shKMT2D-1 and shKMT2D-2). Unpaired t-test *p < 0.05, **p < 0.01, and ***p<0.001. (**J**) Representative images and quantification of invaded HMEL-BRAF^{V600E} cells stably transfected with control or KMT2D shRNAs in Boyden Chamber assay. Unpaired t-test *p < 0.05, **p < 0.01, and ***p<0.001. (**K**) Images of H&E stained and Tyrosinase stained (standard Immunohistochemistry) (40X) melanoma tumors from *iBIP;KMT2D*$^{+/+}$ and *iBIP;KMT2D*$^{L/L}$ mice. Scale bars represent 20 μm. (**L**) Bar graph showing KMT2D expression levels (n=3) in WT-m1, WT-m2, Mut-m1 and Mut-m2 to show loss of KMT2D mRNA. Y-axis represents fold change of KMT2D expression compared to 28S and normalized to average values in WT-m1. (**M**) Immunofluorescence images for KMT2D in WT-m1, WT-m2, Mut-m1, Mut-m2, Mut-m2 + dox (hKMT2D), WT-h1, WT-h2, Mut-h1, Mut-h2, and Mut-h1 + dox (hKMT2D) cells. Nuclear staining is shown by DAPI staining (shown in grayscale). Scale bars represent 20 μm. In (**I**-**J**) and (**L**), data are presented as the mean ± SEM (error bars) of at least three independent experiments or biological replicates.

A

GO DOWNREGULATED iBIP KMT2D MUT VS WT

GO Term	p-value
GO:0007155~cell adhesion	1.7e-10
GO:0009611~response to wounding	1.3e-8
GO:0042445~hormone metabolic process	6.3e-7
GO:0006954~inflammatory response	3.5e-5
GO:0000904~cell morphogenesis involved in differentiation	1.7e-4

B

HALLMARK ALL iBIP KMT2D MUT VS WT

NAME	NOM p-val	FDR q-val
HALLMARK_INTERFERON_GAMMA_RESPONSE	0.0E+00	0.0E+00
HALLMARK_INTERFERON_ALPHA_RESPONSE	0.0E+00	0.0E+00
HALLMARK_HYPOXIA	0.0E+00	0.0E+00
HALLMARK_MYOGENESIS	0.0E+00	1.3E-02
HALLMARK_TNFA_SIGNALING_VIA_NFKB	0.0E+00	1.3E-02
HALLMARK_IL6_JAK_STAT3_SIGNALING	6.0E-03	1.3E-02
HALLMARK_EPITHELIAL_MESENCHYMAL_TRANSITION	4.0E-03	4.9E-02
HALLMARK_GLYCOLYSIS	8.2E-03	8.4E-02
HALLMARK_WNT_BETA_CATENIN_SIGNALING	4.6E-02	9.3E-02
HALLMARK_UV_RESPONSE_DN	4.5E-02	1.8E-01

C

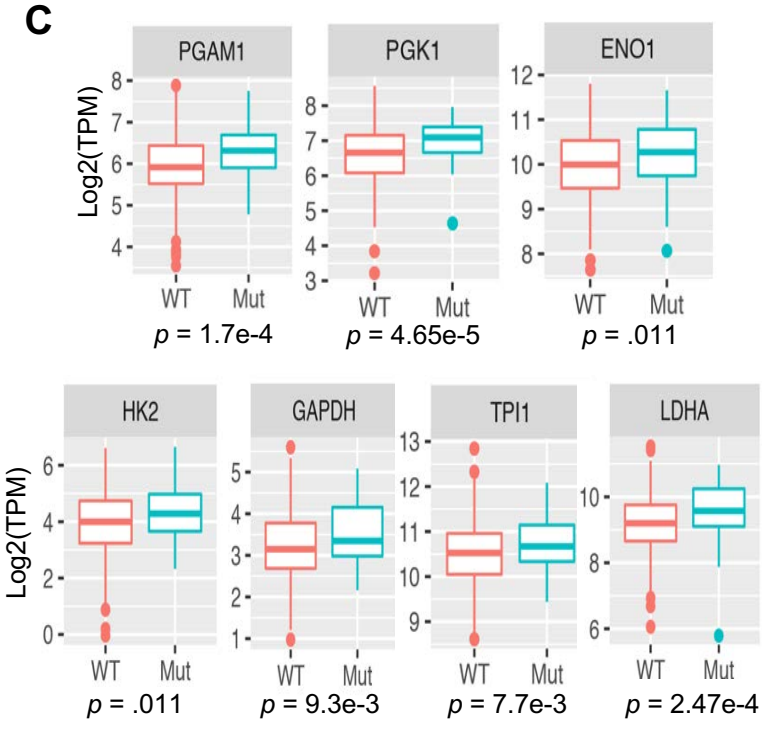

D

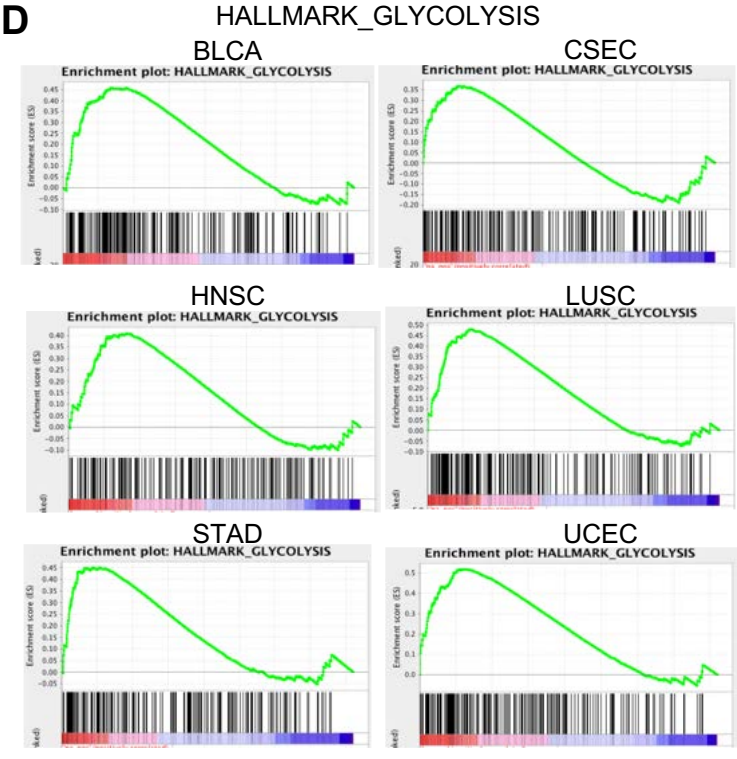

E

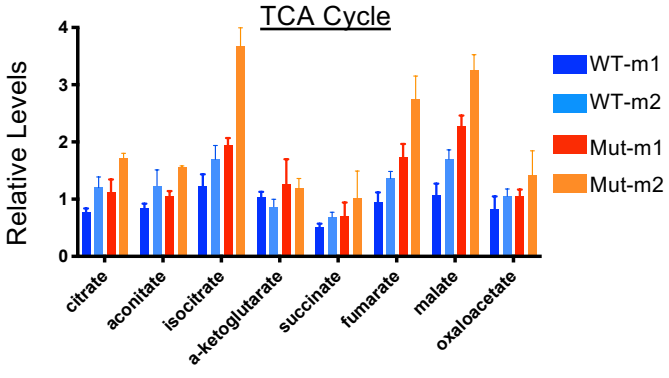

F

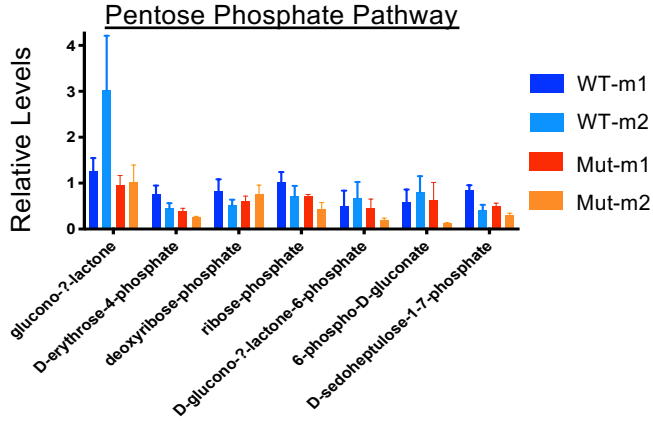

G

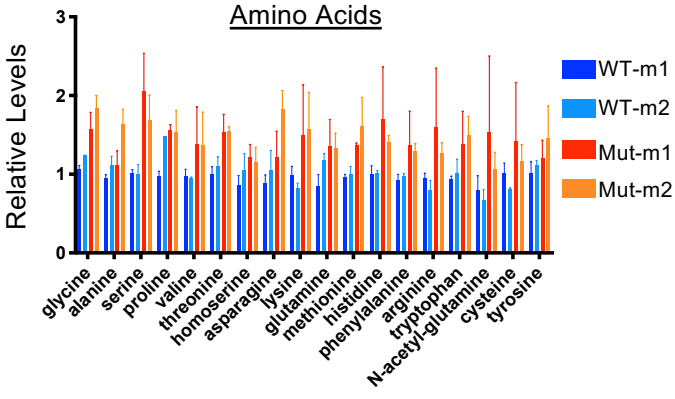

H

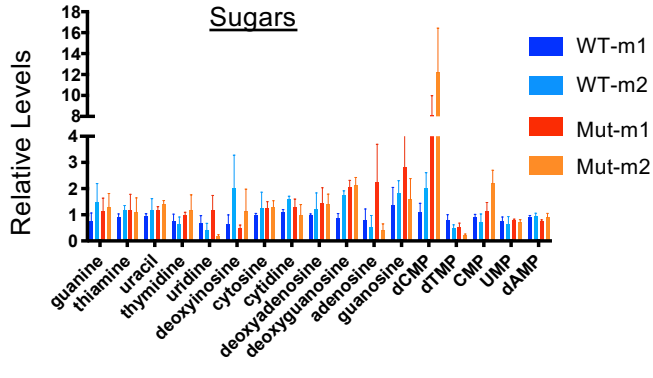

Figure S3, related to **Figure3: KMT2D mutant cells induce energy metabolism pathways and depend on glucose availability.** (**A** and **B**)**.** Top 5 GO terms **(A**) and all significant HALLMARK terms for downregulated genes (FDR < 0.05, FC >2) (**B**) between KMT2D mutant murine cells and KMT2D wild type cells by total RNA-Seq analysis. (**C**) Box plot showing differential expression of multiple glycolysis enzymes in KMT2D mut (n=15) vs WT metastatic melanoma samples (n=15, RPKM > 10) from the TCGA study. p-values represent wilcoxon rank sum test. The bottom and the top rectangles indicate the first quartile (Q1) and third quartile (Q3), respectively. The horizontal lines in the middle signify the median (Q2), and the vertical lines that extend from the top and the bottom of the plot indicate the maximum and minimum values, respectively. **(D)** Enrichment plots for HALLMARK glycolysis pathway in differentially expressed genes between between KMT2D mutant (carrying truncation, frameshift and post4700aa missense) and wild type human tumors from six different tumor types in TCGA data where n of mutant samples > 10. (**E-H**)**.** Bar chart showing relative levels of metabolites (N=3) in the TCA cycle (**E**), pentose phosphate pathway (**F**), amino acids (**G**) and sugars (**H**) in KMT2D WT (WT-m1 and WT-m2) or mutant (Mut-m1 and Mut-m2) tumor-derived murine cell lines. Data are presented as the mean ± SEM (error bars) of at least three independent experiments or biological replicates.

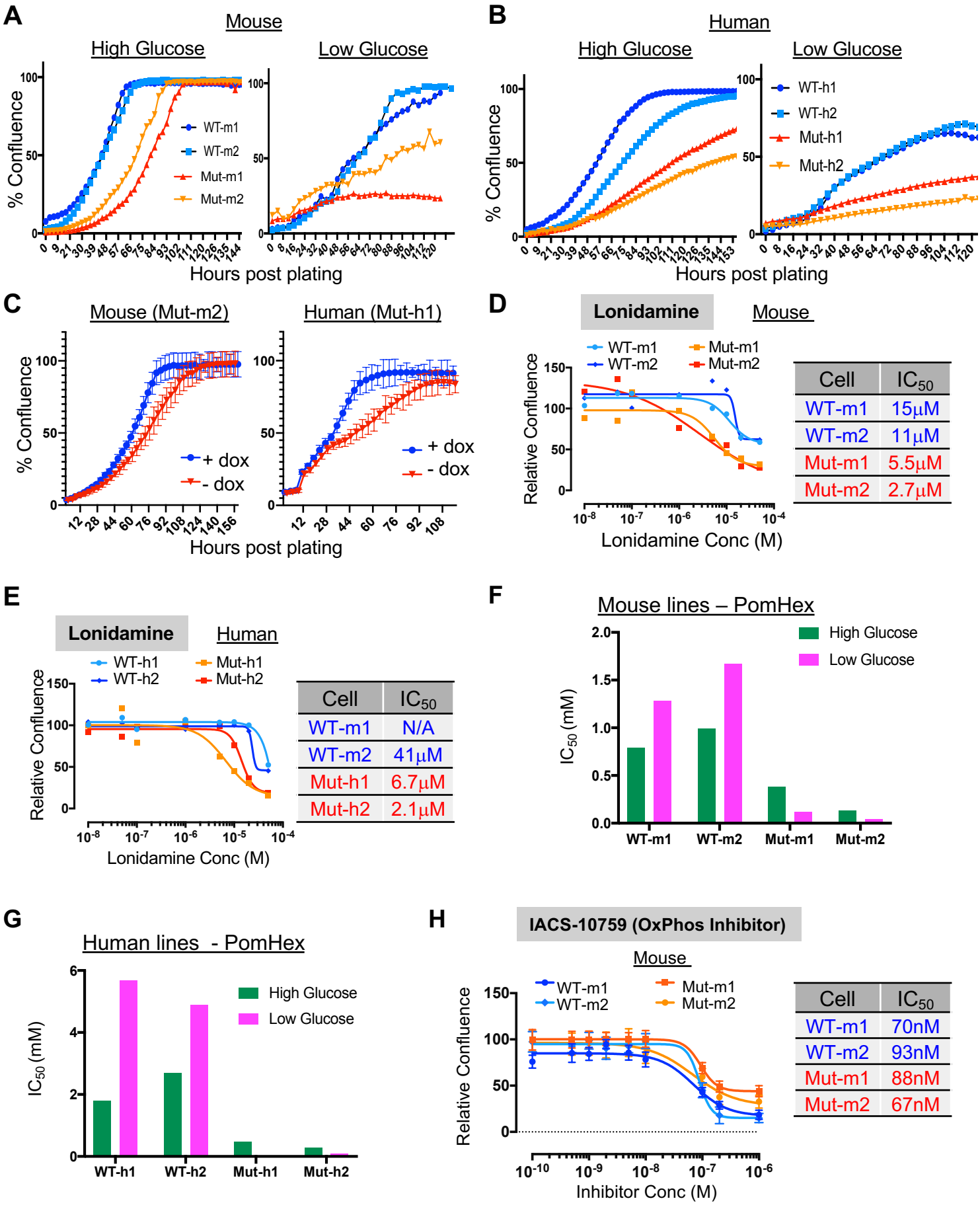

Figure S4, related to **Figure 4: Inhibition of glycolysis preferentially impacts KMT2D mutant cells.** (**A** and **B**) Growth curves for WT-m1, WT-m2, Mut-m1 and Mut-m2 cells (**A**) and WT-h1, WT-h2, Mut-h1, Mut-h2 cells (**B**) in high glucose (4g/L) and low glucose (1g/L) media. X-axis represent hours post plating and Y-axis shows percent confluence. (**C**) Growth curves for Mut-m2 (left) and Mut-h1 (right) reconstituted with doxycyclin-inducible KMT2D plasmid. (**D** and **E**). Growth curves for KMT2D mutant and WT murine (**D**) and human (**E**) melanoma cells treated with varying concentrations of Lonidamine. Relative confluence at 96-hours post treatment are plotted and IC50 values are shown in the accompanying table. (**F** and **G**) Bar plot showing IC_{50} values for Pomhex upon treatment of WT-m1, WT-m2, Mut-m1, Mut-m2 (**F**) or WT-h1, WT-h2, Mut-h1, Mut-h2 (**G**) cells in high glucose (4g/L) or low glucose (1g/L) DMEM media. (**H**) Growth curves for KMT2D mutant and WT murine melanoma cells treated with varying concentrations of IACS-10759, an inhibitor of oxidative phosphorylation. Relative confluence at 96-hours post treatment are plotted and IC50 values are shown in the accompanying table.

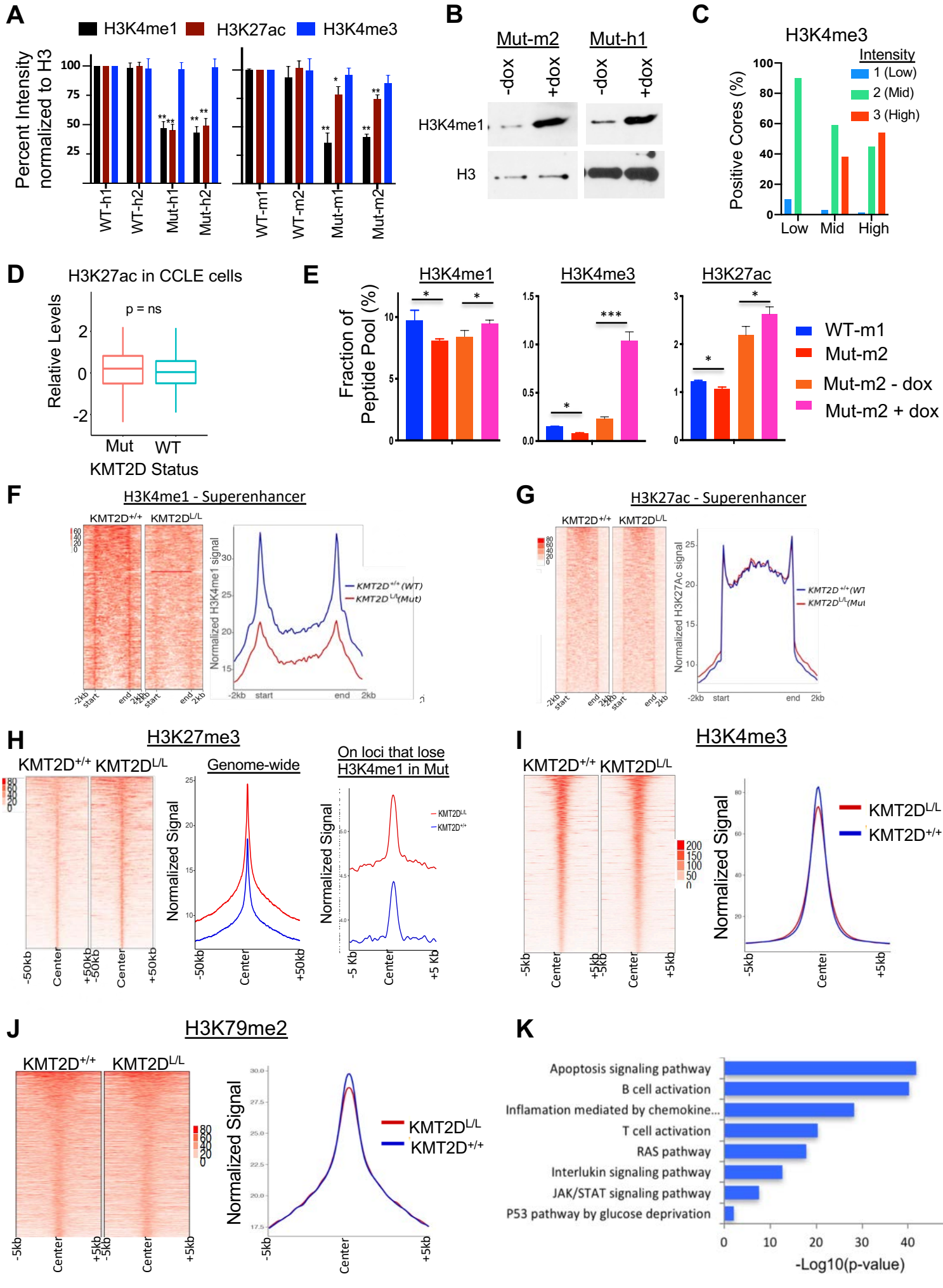
A
H3K4me1
H3K27ac
H3K4me3
Percent Intensity normalized to H3
WT-h1
WT-h2
Mut-h1
Mut-h2
WT-m1
WT-m2
Mut-m1
Mut-m2
B
Mut-m2
Mut-h1
-dox
+dox
H3K4me1
H3
C
H3K4me3
Intensity
1 (Low)
2 (Mid)
3 (High)
Positive Cores (%)
Low
Mid
High
D
H3K27ac in CCLE cells
p = ns
Relative Levels
Mut
WT
KMT2D Status
E
H3K4me1
H3K4me3
H3K27ac
Fraction of Peptide Pool (%)
WT-m1
Mut-m2
Mut-m2 - dox
Mut-m2 + dox
F
H3K4me1 - Superenhancer
KMT2D+/+
KMT2DL/L
Normalized H3K4me1 signal
KMT2D+/+ (WT)
KMT2DL/L (Mut)
G
H3K27ac - Superenhancer
Normalized H3K27Ac signal
H
H3K27me3
Genome-wide
On loci that lose H3K4me1 in Mut
Normalized Signal
I
H3K4me3
J
H3K79me2
K
Apoptosis signaling pathway
B cell activation
Inflamation mediated by chemokine...
T cell activation
RAS pathway
Interlukin signaling pathway
JAK/STAT signaling pathway
P53 pathway by glucose deprivation
-Log10(p-value)

Figure S5, related to **Figure 5: Levels of H3K4me3, H3K27me3 and H3K79me2 in KMT2D WT and mutant melanoma tumors.** (**A**) Quantitation of the western blot (n=3) shown in Figure 5A. **(B)** Western blot showing total H3K4me1 and H3 in KMT2D mutant (Mut-m2, Mut-h1) and rescue with hKMT2D (+dox) murine (left) and human (right) melanoma cells. **(C)** Bar chart showing percent positive cores of shown H3K4me3 staining (scored numerically as 1, 2, 3) for three categories defined by KMT2D expression as Low (score of 1 or 1.5, n = 10 mid (score of 2, n = 57) and high (score of 3, n = 33). **(D)** Relative levels of H3K27ac from histone modification mass spectrometry data in KMT2D mutant (n=126) or WT (n = 293) cell lines in the CCLE data base. The bottom and the top rectangles indicate the first quartile (Q1) and third quartile (Q3), respectively. The horizontal lines in the middle signify the median (Q2), and the vertical lines that extend from the top and the bottom of the plot indicate the maximum and minimum values, respectively. **(E)** Mod-spec (active motif) based quantitation of H3K4me1, H3K27ac and H3K4me3 in KMT2D WT and mutant murine tumor-derived melanoma cells (WT-m1 and Mut-m2). Data are presented as the mean ± SEM (error bars) of at least three independent experiments or biological replicates. **(F** and **G)**. Heat map (left panels) and average intensity curves (right panels) for super-enhancer peaks based on H3K4me1 (**F**) and H3K27ac (**G**) ChIP-Seq data peak in *iBIP;KMT2D*$^{+/+}$ and *iBIP;KMT2D*$^{L/L}$ melanoma tumors. (**H-J)** Heat map (left panels) and average intensity curves (right panels) derived from the ChIP-Seq reads (RPKM) for H3K27me3 (**H**), H3K4me3 (**I**) and H3K79me2 (**J**) at enriched promoters in 10kb window centered on the middle of the peak in *iBIP;KMT2D*$^{+/+}$ and *iBIP;KMT2D*$^{L/L}$ melanoma tumors. Signals show enrichment in the specific peaks for these marks in respective type of tumor. In **H**, right panel shows H3K27me3 signal on loci that lose H3K4me1 in KMT2D mut vs WT. (**K)** Pathway analysis for active enhancer (H3K4me1 and H3K27ac overlap) peaks specific to KMT2D mutant compared to KMT2D wild type tumors.

A

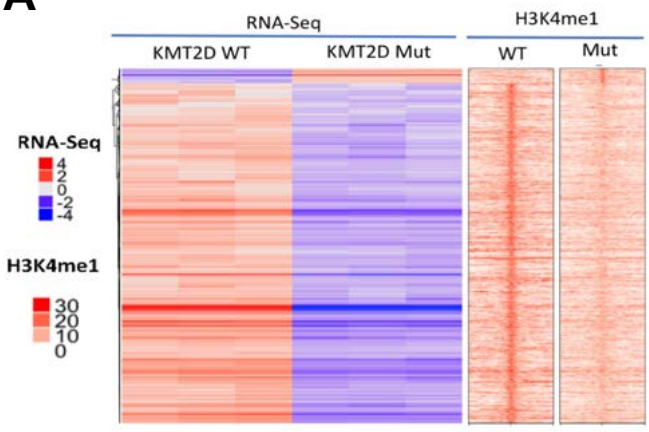

B

GO Terms	p-value
GO:0016310~phosphorylation	7.73E-10
GO:0035556~intracellular signal transduction	2.47E-09
GO:0006897~endocytosis	1.53E-08
GO:0006468~protein phosphorylation	6.13E-08
GO:0070374~positive regulation of ERK1 and ERK2 cascade	1.45E-06
GO:0006469~negative regulation of protein kinase activity	3.60E-06
GO:0050731~positive regulation of peptidyl-tyrosine phospl	8.84E-06
GO:0006605~protein targeting	2.78E-05
GO:0030036~actin cytoskeleton organization	3.23E-05
GO:0016477~cell migration	4.98E-05

C

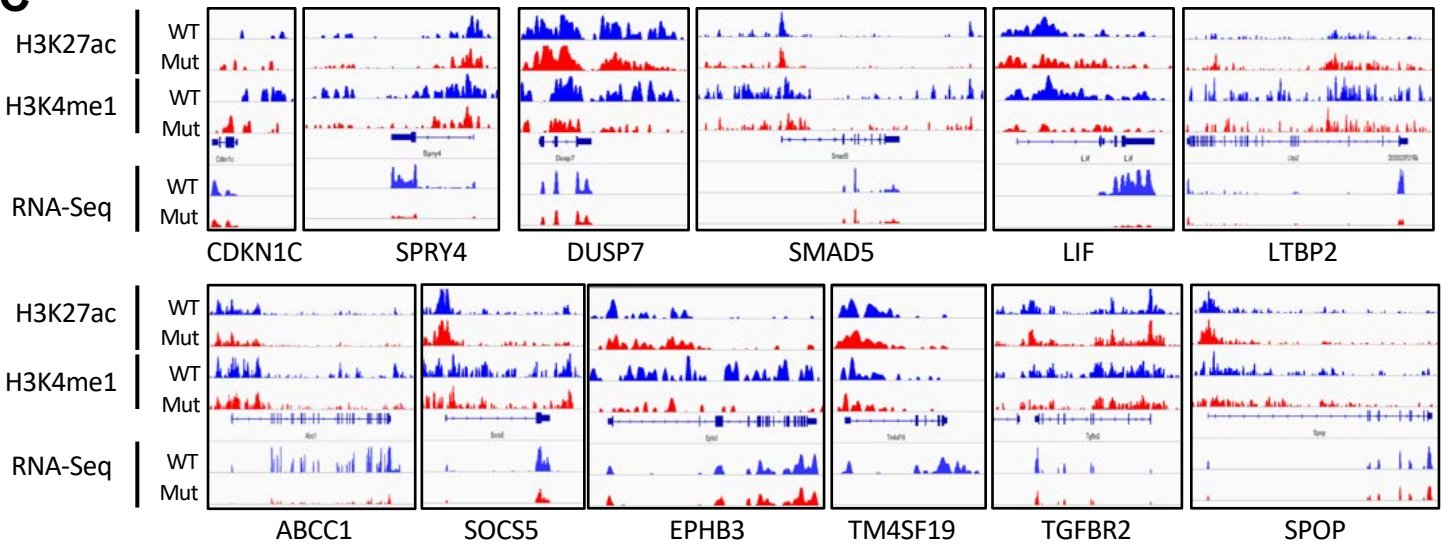

D

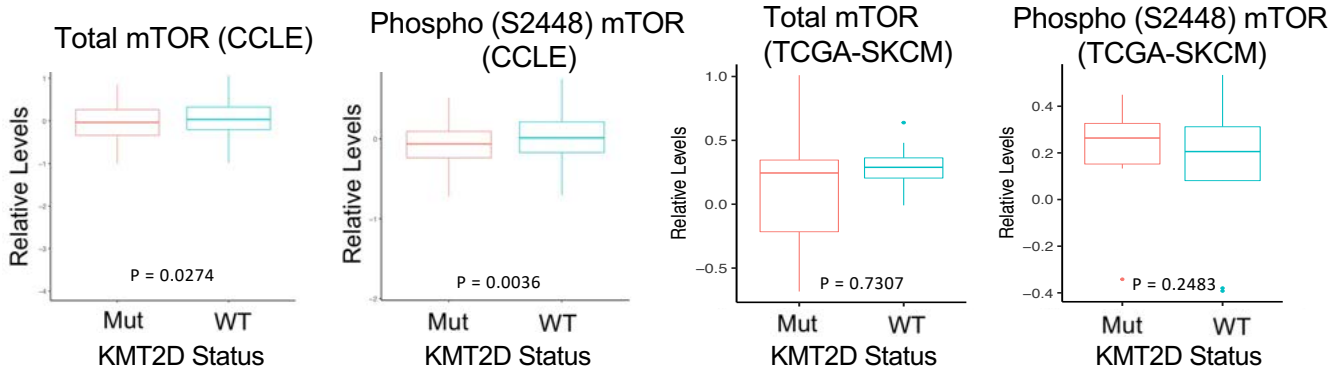

E

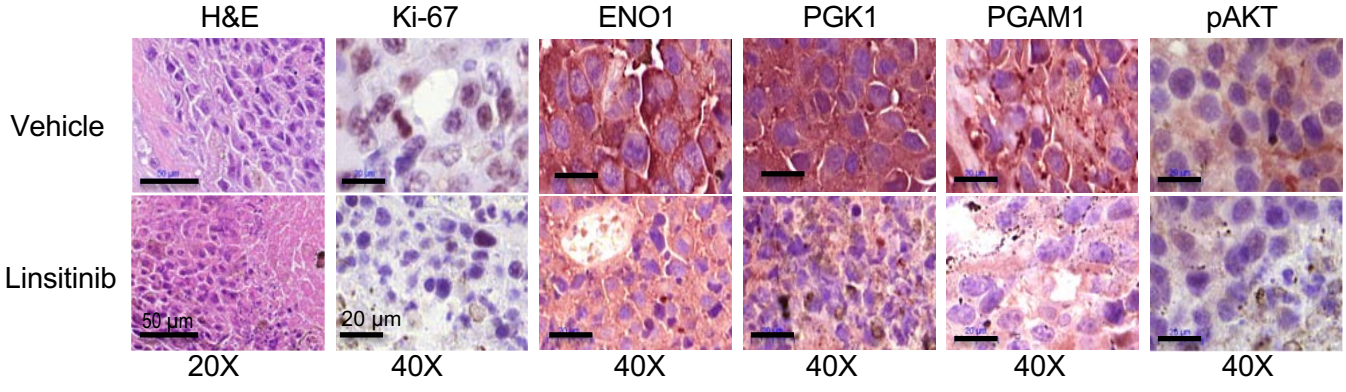

Figure S6, related to **Figure 6: IGF signaling and aberrantly activates glycolysis in KMT2D mutant melanoma tumors.** (**A**) Heat maps showing differentially expressed genes and associated H3K4me1 signals in the vicinity as noted. R1, R2 and R3 refer to three replicates for WT-m1 and Mut-m2 cells. (**B**) All significant GO terms for genes which are differentially expressed and harbor loss of H3K4me1 mark at associated loci in KMT2D mutant melanoma cells compared to WT tumor cells. **(C)** Snapshots of IGV viewer for H3K4me1, H3K27ac and RNA-Seq signals on genomic loci surrounding various *bona fide* or putative tumor suppressor genes in KMT2D wild type or mutant tumors. (**D**) Box plots showing relative levels of total mTOR or phosphorylated form (S2448) in KMT2D mutant vs WT cells using CCLE RPPA data (Mut, n= 123; WT, n = 290) (left panels) and TCGA SKCM tumors RPPA data (n = 15) (right panels). The bottom and the top rectangles indicate the first quartile (Q1) and third quartile (Q3), respectively. The horizontal lines in the middle signify the median (Q2), and the vertical lines that extend from the top and the bottom of the plot indicate the maximum and minimum values, respectively. **(E)** Images of H&E stained tumor or those stained for the product of three glycolysis genes (ENO1, PGK1 and PGAM1) or pAKT in xenograft tumors of Mut-m2 cells treated with vehicle or Linsitinib (20mg/kg). Magnification is shown below the images. Scale bar shows 20 μm in all cases except H&E images where it represents 50 μm.

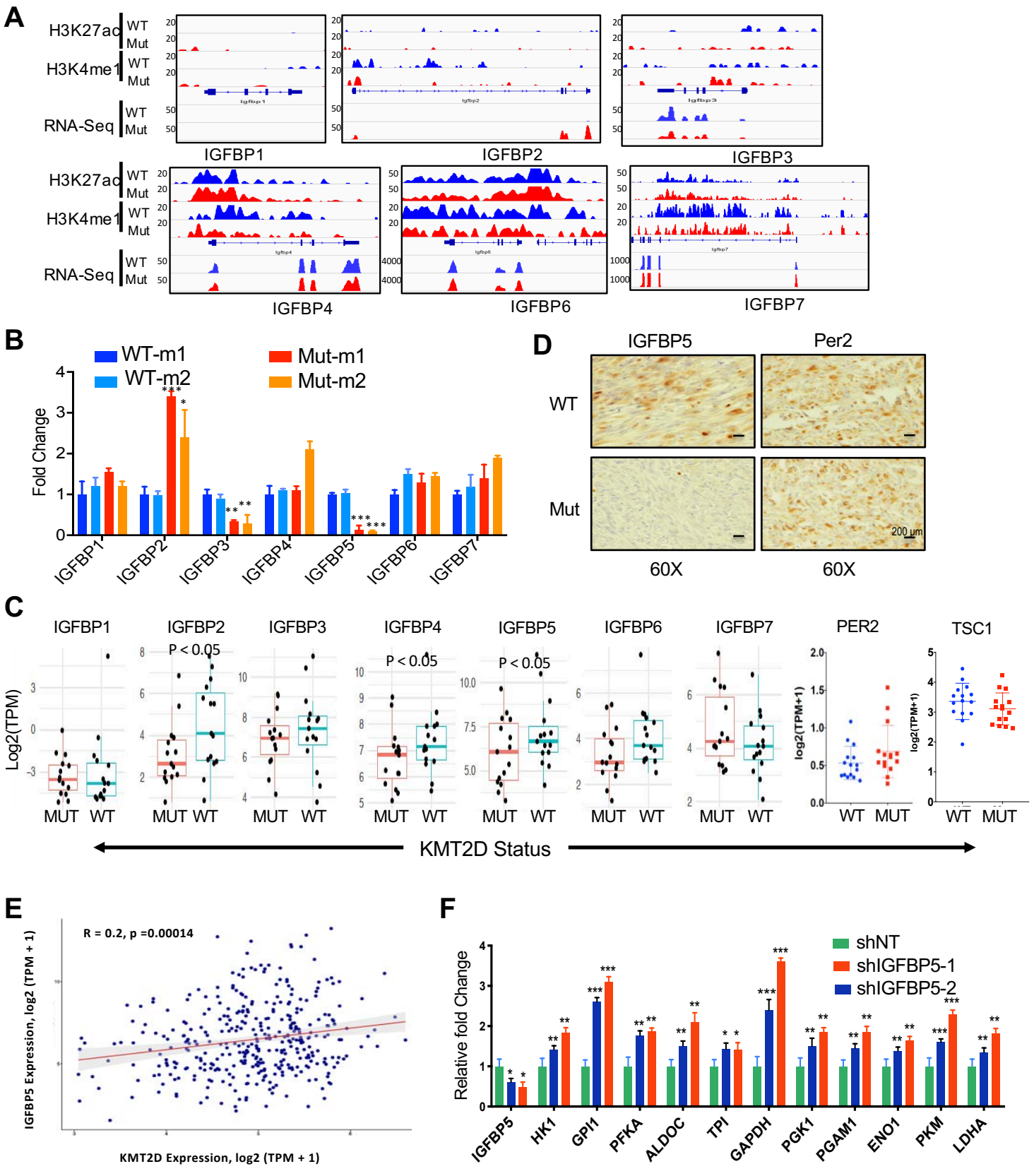

Figure S7, related to **Figure 7**: **Loss of enhancer activity at IGFBP5 mediates activation of IGF signaling and aberrantly activates glycolysis in KMT2D mutant melanoma tumors.** (**A**) IGV snapshot showing RNA-seq, H3K27Ac, H3K4me1 signal tracks for genomic locus around with IGFBP genes. (**B**) Bar graph showing relative expression levels (n=3) of indicated IGFBP genes in murine KMT2D mutant (Mut-m1 and Mut-m2) and WT (WT-m1 and WT-m2) cells. Y-axis represents fold change of the gene expression compared to 28S and normalized to control shRNA samples. Standard t-test *p < 0.05, **p < 0.01, ***p < 0.001. (**C**) Box plot showing expression of IGFBP genes, Per2 and TSC1 in the melanoma TCGA samples that harbor functional mutations (nonsense, frameshift or post4700aa) (n = 15) or WT copies for KMT2D (n = 15). The bottom and the top rectangles indicate the first quartile (Q1) and third quartile (Q3), respectively. The horizontal lines in the middle signify the median (Q2), and the vertical lines that extend from the top and the bottom of the plot indicate the maximum and minimum values, respectively. (**D**) Images of H&E stained tumor for those stained for the product of IGFBP5 or Per2 *in iBIP-Kmt2d*$^{+/+}$ (WT) and *iBIP-Kmt2d*$^{L/L}$ (Mut) tumors. Magnification is shown below the images. Scale bar is 200 µm. (**E**) Correlation plot between KMT2D (X-axis) and IGFBP5 (Y-axis) mRNA expression in all KMT2D WT metastatic melanoma tumors (n=254) from the TCGA study. (**F**) Bar chart showing relative fold change of mRNA expression (n=3) of IGFBP5 and indicated glycolysis enzymes in WT-m1 cells infected with IGFBP5 shRNAs (shIGFBP5-1 and shIGFBP5-2) or control shRNA (shNT). Data was normalized to 28s values and converted to fold change considering shNT values as 1. Standard t-test *p < 0.05, **p < 0.01, ***p < 0.001. In (**B**) and (**F**), data are presented as the mean ± SEM (error bars) of at least three independent experiments or biological replicates.